

Unified Approach to Power-Efficiency Trade-Off of Generic Thermal Machines

Yu-Han Ma^{1,2,*} and Cong Fu^{1,3,†}

¹Department of Physics, Beijing Normal University, Beijing, 100875, China

²Graduate School of China Academy of Engineering Physics, Beijing, 100193, China

³Department of Physics, Xiamen University, Xiamen 361005, Fujian, China

(Dated: November 7, 2024)

Due to the diverse functionalities of different thermal machines, their optimization relies on a case-by-case basis, lacking unified results. In this work, we propose a general approach to determine power-efficiency trade-off relation (PETOR) for any thermal machine. For cases where cycle (of duration τ) irreversibility satisfies the typical $1/\tau$ -scaling, we provide a unified PETOR which is applicable to heat engines, refrigerators, heat exchangers and heat pumps. It is shown that, some typical PETORs, such as those for low-dissipation Carnot cycles (including heat engine and refrigerator cycles) and the steady-state heat engines operating between finite-sized reservoirs are naturally recovered.

Introduction.— Finite-time thermodynamics bridges the gap between the idealized quasi-static thermodynamic cycle described by equilibrium thermodynamics and the practical thermal machines operating within finite cycle times [1, 2]. Quantitatively, the performance of finite-time thermodynamic cycles is completely characterized by power-efficiency trade-off relation (PETOR) [3–10], a consequence of the energy dissipation inherent in the cycle’s irreversibilities [5, 11–13]. In previous studies, various PETORs have been derived with different theoretical frameworks, such as PETOR for endoreversible Carnot heat engine [3], PETOR for linear irreversible heat engines [4, 9], and PETOR for low-dissipation heat engine [6, 7]. Besides, one key parameter of finite-time thermal machines, the efficiency at maximum power [14–18], stands out as a typical point on the power-efficiency tradeoff curve [7, 19–21], delineating the energy conversion efficiency when the power is maximized.

Regarding the quest for completeness and universality in the description and optimization for practical thermal machines, there are two critical limitations in the existing studies: i) In contrast to the rich studies on PETORs for heat engines, discussions on the PETORs for refrigerators and heat pumps remain relatively scarce [22, 23]; ii) Some studies attempt to develop a generalized approach for optimizing various thermal machines [24–27], although the proposed methods are general in some sense, specific optimizations still require the identification the particular machine before implementation. Note that parameters characterizing thermal machine’s performance, such as output power and energy conversion efficiency, are determined by specific design functions, with entirely different definitions for different machines. For instance, concerning energy conversion efficiency, the coefficient of performance(COP) for refrigerators [28] and heat pumps [29] the efficiency for heat engines have distinct definitions. In this sense, it seems unlikely to obtain a unified PETOR for general thermodynamic cycles, necessitating optimize different thermal machines on a case-by-case basis.

Our purpose in this Letter is to formulate a unified power-efficiency trade-off applicable to any thermal machine, free

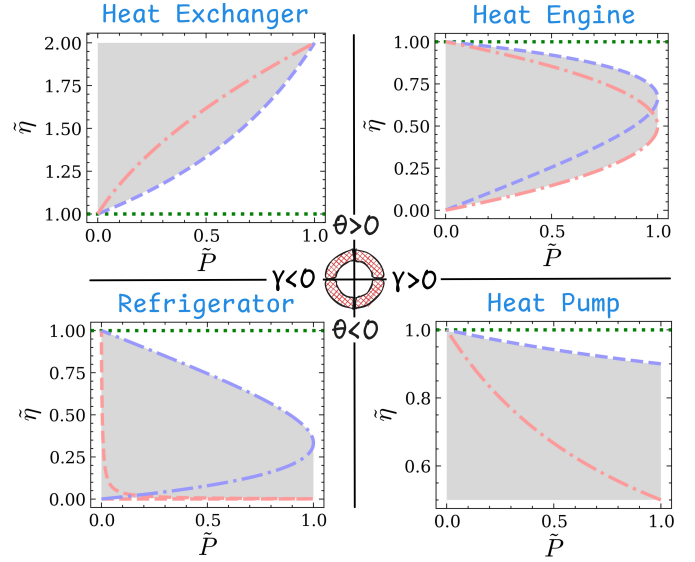


FIG. 1. The normalized power-efficiency trade-off relation of four typical thermal machines operating between two reservoirs of temperatures $T_c/T_h = 0.5$. The blue dashed (red dash-dotted) curve represents Eq. (1) with the dissipation ratio $\delta \rightarrow 1$ ($\delta \rightarrow 0$), the normalized reversible efficiency $\tilde{\eta} = 1$ is plotted with the green dotted line, and the shadow area marks the available operation region of the machine.

from restriction imposed by inconsistent definitions of performance parameters for different machines, thus overcoming the aforementioned limitations. By connecting the geometric lower bound of irreversibility for non-equilibrium thermodynamic cycles [11] with thermal machine performance parameters, which are uniformly described with a pair of independent sign functions associated with the cycle direction and machine function. We succinctly obtain the PETOR for a generic thermal machine (whose specific features are determined a coefficient χ) operating in the slow-driving regime as

$$\tilde{P} \leq \frac{4\tilde{\eta}(1-\tilde{\eta})(1-\chi\eta_{\text{rev}})}{(1-\chi\tilde{\eta}\eta_{\text{rev}})^2}, \quad (1)$$

where $\tilde{P} \equiv P/P_{\text{max}}$ and $\tilde{\eta} \equiv \eta/\eta_{\text{rev}}$ are the normalized power and efficiency, respectively. P_{max} is the maximum output

* yhma@bnu.edu.cn

† fucong@stu.xmu.edu.cn

power of the machine whose reversible efficiency is denoted as η_{rev} . This result is applicable to heat engines, refrigerators, heat pump, and heat exchanger cycles operating between arbitrary number of heat reservoirs, thereby contributing a unifying perspective on power-efficiency trade-off in finite-time thermodynamics. In Fig. 1, we illustrated the PETORs in different regions of θ and γ (see Tab. I).

TABLE I. Cycle quantities of typical thermal machines

	θ	γ	O	I	η	P
Heat Engine	+1	+1	W	Q^h	W/Q^h	W/τ
Heat Exchanger	+1	-1	Q^c	Q^h	Q^c/Q^h	Q^c/τ
Refrigerator	-1	-1	Q^c	W	Q^c/W	Q^c/τ
Heat Pump	-1	+1	Q^h	W	Q^h/W	Q^h/τ

Unified thermodynamic performance tradeoff.— Typical thermal machines, including heat engines, heat exchangers [30], refrigerators, and heat pumps, are designed to convert energy in various forms according to actual demands. Among them, heat engines harness the temperature difference between hot and cold heat reservoirs to perform work. Both refrigerators and heat pumps create heat flow from cold reservoirs to hot reservoirs through work input, one for cooling and the other for heating. In general sense, the energy conversion efficiency of any thermal machine can be defined as $\eta \equiv O/I$, where O and I are respectively the energy exchange at the input end and output end of the machine, as illustrated in Tab. I [30]. It should be mentioned here that "output" is categorized from the perspective of the machine's function, not necessarily the direction of energy flow. For instance, for a general heat engine cycle illustrated in Fig. 2(a), its output function is performing work externally, O represents work output W and I represents total heat absorption $Q^h = \sum_j Q^{h,j}$ with $Q^{h,j}$ the heat absorption from the j -th hot reservoir (We do not restrict the number N of reservoirs, and the following discussion is applicable to any situation with $N \geq 2$). In this case, the direction of energy flow at the output side of the machine is also from the machine to the external environment. However, for a refrigerator cycle, where the output function is absorbing heat from the low-temperature end, namely the direction of energy flow is from the surroundings to the refrigerator. For thermal machines operating within finite cycle time, by dividing O(I) into reversible part $O_{\text{rev}}(I_{\text{rev}})$ and irreversible part $A_o(A_i)$, we further express the machine efficiency as

$$\eta = \frac{O_{\text{rev}} - \theta \gamma A_o}{I_{\text{rev}} - \theta A_i}. \quad (2)$$

Here, O_{rev} , I_{rev} , and $A_{o/i}$ are all positive. $\theta = \pm 1$ is a sign function determined by the direction of the cycle, while $\gamma = \pm 1$ is another sign function determined by the specific function of the machine with a given θ , as illustrated in Tab. I. In Fig 2(b), a clockwise ($\theta > 0$) and a counterclockwise ($\theta < 0$) finite-time Carnot cycle between two reservoirs of temperatures $T_h > T_c$ is depicted, where J -axis indicates the direction of energy flow exiting the cycles. In such a geometric repre-

sentation, the greater the output power of the cycle, the further away it is from the plane of $J = 0$.

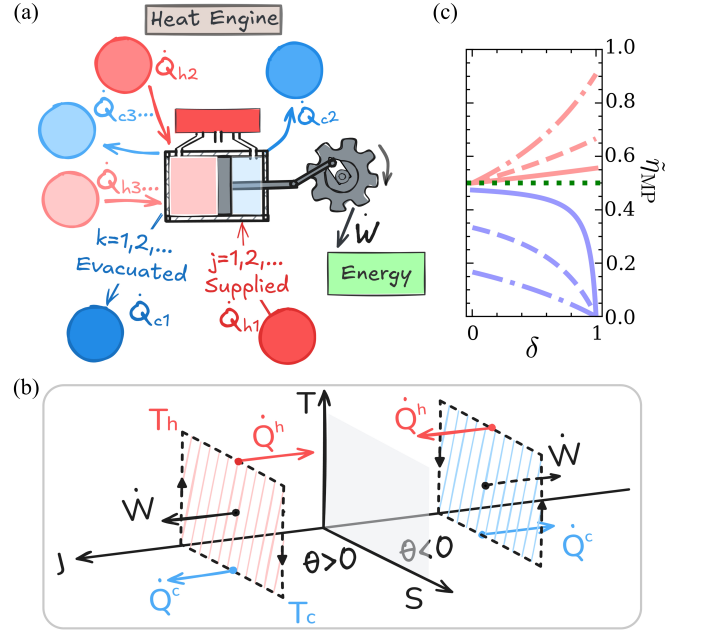


FIG. 2. (a) schematic of a heat engine operates among multiple heat reservoirs which is represented by red and blue circles. The engine extracts from supplied reservoirs and releases to others. (b) Temperature-entropy ($T - S$) diagram of clockwise and counterclockwise finite-time Carnot cycles. The orientation of the J -axis represents the direction of energy flow from the cycles to the heat reservoirs. (c) EMPs of heat engine ($\tilde{\eta}_{\text{MP}} \geq 0.5$) and refrigerator ($\tilde{\eta}_{\text{MP}} \leq 0.5$) as functions of δ . In this example with two reservoirs of temperatures $T_c < T_h$, dash-dotted curve, dashed curve, and solid curve are plotted with $T_c/T_h = 0.1, 0.5, 0.8$, respectively.

TABLE II. Dissipation and its ratio associated with input and output ends of typical thermal machines

	A_o	A_i	A	A_o/A	A_i/A
Heat Engine	W_{ir}	Q_{ir}^h	W_{ir}	1	δ
Heat Exchanger	Q_{ir}^c	Q_{ir}^h	W_{ir}	$1 - \delta$	δ
Refrigerator	Q_{ir}^c	W_{ir}	W_{ir}	$1 - \delta$	1
Heat Pump	Q_{ir}^h	W_{ir}	W_{ir}	δ	1

The dissipation W_{ir} in the work output/input process, denoted as A , is contributed by all heat transfer processes together [31]. For typical thermal machines, we illustrate the dissipation in different processes in Tab. II, where the dissipation ratios of different processes are determined with the definition $\delta \equiv Q_{\text{ir}}^h/W_{\text{ir}} \in [0, 1]$. Taking use of the cycle parameters, we can unify A_o and A_i in terms of A as

$$A_i = \delta^{\frac{1+\theta}{2}} A, \quad A_o = (1 - \delta)^{\frac{1-\gamma}{2}} \delta^{\frac{(1-\theta)(1+\gamma)}{4}} A. \quad (3)$$

Then Eq. (2) becomes

$$\eta = \frac{O_{\text{rev}} - \theta \gamma (1 - \delta)^{\frac{1-\gamma}{2}} \delta^{\frac{(1-\theta)(1+\gamma)}{4}} A}{I_{\text{rev}} - \theta \delta^{\frac{1+\theta}{2}} A}, \quad (4)$$

such that we can rewrite A in term of η as

$$A = \frac{\chi(O_{\text{rev}} - I_{\text{rev}}\eta)}{\theta\gamma(1 - \chi\eta)\delta^{\frac{1+\theta}{2}}}, \quad (5)$$

where

$$\chi \equiv \gamma(1 - \delta)^{\frac{\gamma-1}{2}} \delta^{\left[\theta - \frac{(1-\theta)(\gamma-1)}{4}\right]} \quad (6)$$

Physically, it is reasonable to assume that A has a cycle duration τ -dependent lower bound, i.e., $A \geq A_{\text{min}}(\tau)$. By further noticing the output power of the machine is $P = O/\tau$, Eq. (5) yields

$$\frac{\chi(O_{\text{rev}} - I_{\text{rev}}\eta)}{\theta\gamma(1 - \chi\eta)\delta^{\frac{1+\theta}{2}}} \geq A_{\text{min}}(\tau) = A_{\text{min}}\left(\frac{O}{P}\right). \quad (7)$$

Eliminating $O = O_{\text{rev}} - \theta\gamma A_o$ from the right side of the above equation with Eqs. (3) and (5), an general inequality with respect to P and η is obtained.

Specifically, in the slow-driving regime, the minimal energetic dissipation is proved to be $A_{\text{min}} = \mathcal{L}^2/\tau$ [11], where \mathcal{L} is the thermodynamic length in thermodynamic geometry theory. This low bound for irreversibility is achieved when the driving protocol of the cycle maintains uniform speed along the thermodynamic length trajectory (in the parametric space defined by thermodynamic state variables) [11, 32, 33]. With this typical $1/\tau$ -scaling, Eq. (7) becomes

$$\frac{\chi(O_{\text{rev}} - I_{\text{rev}}\eta)}{\theta\gamma(1 - \chi\eta)\delta^{\frac{1+\theta}{2}}} \geq \frac{\mathcal{L}^2 P}{O} = \frac{\mathcal{L}^2 P}{O_{\text{rev}} - \theta\gamma A_o}, \quad (8)$$

substituting Eqs. (3) and (5) into which, by straightforward calculation, we find the Unified trade-off relation between power and efficiency as

$$P \leq \left(\frac{I_{\text{rev}}}{\mathcal{L}}\right)^2 \frac{\eta(\eta_{\text{rev}} - \eta)(1 - \chi\eta_{\text{rev}})}{\theta\delta^{\frac{1+\theta}{2}}\chi^{-1}(1 - \chi\eta)^2} \equiv P_m(\eta), \quad (9)$$

where $\eta_{\text{rev}} = O_{\text{rev}}/I_{\text{rev}}$ is the reversible efficiency. For a given efficiency, the power attains a maximum value when the cycle dissipation is minimized. By solving $dP_m(\eta)/d\eta = 0$, the maximum power P_{max} and the corresponding EMP η_{MP} are obtained as

$$\eta_{\text{MP}} = \frac{\eta_{\text{rev}}}{2 - \chi\eta_{\text{rev}}} \quad (10)$$

and

$$P_{\text{max}} = \theta\gamma \left(\frac{I_{\text{rev}}\eta_{\text{rev}}}{2\mathcal{L}}\right)^2 \delta^{-\frac{1+\theta}{2}} |\chi|. \quad (11)$$

Normalize Eq. (9) with P_{max} and η_{rev} , the main result of this Letter, Eq. (1), is obtained. We make two remarks here:

i) the $1/\tau$ -scaling of dissipation can also be derived using the framework of linear irreversible thermodynamics [9, 34], hence our results are applicable to steady-state heat engines in liner response regime as well. Besides, utilizing the so-called shortcut to isothermality method [32, 35], the $1/\tau$ -scaling

can be maintained even beyond the slow-driving regime [33], making our results applicable to any thermal machine constructed using shortcut to isothermality and are not limited by driving speed. In the cases where the minimal cycle dissipation deviates from the $1/\tau$ -scaling [36–40], for example, when $A_{\text{min}}(\tau) \propto \tau^\alpha$ with $\alpha < 0$ [36–38], Eq. (7) can directly yield analytical explicit PETOR. For more complex scenarios, with the series expansion of A_{min} respect to τ [39], our approach provides transcendental equation regarding P and η , which will require further numerical calculation to obtain specific tradeoff relation.

iii) Equation (11) indicates that, for thermal machines with $\theta\gamma < 0$ ($\theta = -\gamma = -1$ for heat pumps and $\theta = -\gamma = 1$ for heat exchangers), the maximum power is negative, which is nonphysical. This implies that, under the condition of requiring positive output, the machines with $\theta\gamma < 0$ do not have a locally optimal output power with respect to η , which results in a monotonic dependence of power on efficiency (PETORs with $\theta\gamma < 0$ in Fig. 1). For thermal machines with $\theta\gamma > 0$, the EMPs as functions of δ in the two-reservoirs case is plotted in Fig. 2(b). In this figure, $\tilde{\eta}_{\text{MP}} = \eta_{\text{MP}}/\eta_{\text{rev}} \geq 0.5$ for heat engines while $\tilde{\eta}_{\text{MP}} \leq 0.5$ for refrigerators, different curve styles correspond to different temperature ratios of reservoirs. In addition, Eq. (1) implies that once $\tilde{\eta}$ is fixed, the maximum \tilde{P} is determined. In this scenario, increasing P_{max} can enhance P . As shown in Eq. (11), increasing I_{rev} and decreasing \mathcal{L} can effectively increase P , where the former can be achieved by enlarging the size of the machine (more working substance), and the latter can be realized through optimizing the driving path of the machine cycle [32, 41] or leveraging collective advantages offered by interactions inside working substances [42, 43].

PETORs for heat engines.— By specifying $\theta = 1$ and $\gamma = 1$, one has $\chi = \delta$ from Eq. (6), and thus, it follows from Eq. (1) that, the normalized PETOR for slow-driving heat engines reads

$$\tilde{P} \leq \frac{4\tilde{\eta}(1 - \tilde{\eta})(1 - \delta\eta_{\text{rev}})}{(1 - \delta\eta_{\text{rev}}\tilde{\eta})^2} \quad (12)$$

with $\eta_{\text{rev}} \equiv W_{\text{rev}}/Q_{\text{h}}^{\text{rev}}$ the efficiency of a heat engine operating reversibly. This result is equivalent to that obtained with shortcut strategy [33]. The equal sign of Eq. (12) is saturated with $\delta = \mathcal{L}_{\text{h}}/\mathcal{L}$ (See Appendix A for an example of ideal gas), where \mathcal{L}_{h} is the total thermodynamic length contributed by all heat absorption processes [33]. In addition, according to Eq. (10), we obtain the EMP as

$$\eta_{\text{MP}} = \frac{\eta_{\text{rev}}}{2 - \delta\eta_{\text{rev}}}, \quad (13)$$

with $P_{\text{max}} = (W_{\text{rev}}\mathcal{L}^{-1})^2/4$ the corresponding maximum power. Obviously from Eq. (13) we have $\eta_{\text{rev}}/2 \leq \eta_{\text{MP}} \leq \eta_{\text{rev}}/(2 - \eta_{\text{rev}})$. This is consistent with the results obtained in Ref. [33, 44, 45].

When the scenario is further restricted to only two heat baths, a high-temperature one with temperature T_{h} and a low-temperature one with temperature T_{c} , the reversible efficiency simplifies to its Carnot form, namely, $\eta_{\text{rev}} = \eta_{\text{C}} = 1 - T_{\text{c}}/T_{\text{h}}$.

In this case, Eq. (13) is simplified as $\eta_C/(2 - \delta\eta_C)$ (see Fig. 2(b)), recovering the EMP of low-dissipation Carnot engine obtained by Esposito et al. [17]. Beside, by taking $\delta = 1$, the overall upper bound for efficiency at arbitrary given power is obtained from Eq. (12) as (See Appendix B for details)

$$\tilde{\eta}_U = 1 - \frac{(1 - \eta_C)\tilde{P}}{2(1 + \sqrt{1 - \tilde{P}}) - \tilde{P}\eta_C}, \quad (14)$$

and the overall lower bound, $\tilde{\eta}_L = (1 - \sqrt{1 - \tilde{P}})/2$, is achieved with $\delta = 0$. These bounds have been obtained before with different approaches [4, 6, 7] and experimentally tested [13]. Furthermore, in the case of two finite-sized heat reservoirs, the quasi-static efficiency of the heat engine is referred to as efficiency at maximum work (η_{MW}) [46, 47]. In this scenario, it can be easily verified that Eq.(12) is consistent with the result obtained with linear irreversible thermodynamics, as given by [Eq. (10)] of Ref. [9]. The EMP of the engine satisfies $\eta_{MW}/2 \leq \eta_{MP} \leq \eta_{MW}/(2 - \eta_{MW})$ [9, 34]. We do not delve into detailed discussions on this issue here.

PETORs for refrigerators.— For refrigerators, their efficiency is referred to as the Coefficient of Performance (COP), typically denoted by the symbol ε . It follows from Eq. (1) that, by specifying $\theta = -1$ and $\gamma = -1$, i.e., $\chi = -(1 - \delta)^{-1}$, and using variable substitution $\eta \rightarrow \varepsilon$ and $\eta_{rev} \rightarrow \varepsilon_{rev}$, the PETOR for slow-driving refrigerators is obtained as

$$\tilde{P} \leq \frac{4\tilde{\varepsilon}(1 - \tilde{\varepsilon})[1 + (1 - \delta)^{-1}\varepsilon_{rev}]}{[1 + (1 - \delta)^{-1}\varepsilon_{rev}\tilde{\varepsilon}]^2}, \quad (15)$$

where $\varepsilon_{rev} \equiv Q_{rev}^c/W_{rev}$ represents the COP a refrigerator operating reversibly. In this situation, the efficiency at maximum cooling power and corresponding maximum cooling power follows

$$\varepsilon_{MP} = \frac{\varepsilon_{rev}}{2 + (1 - \delta)^{-1}\varepsilon_{rev}}, P_{max} = \frac{(1 - \delta)^{-1}}{4} \left(\frac{W_{rev}\varepsilon_{rev}}{\mathcal{L}} \right)^2, \quad (16)$$

respectively. Since $(1 - \delta)^{-1} \in [1, \infty)$, the EMP of refrigerators satisfy $0 \leq \varepsilon_{MP} \leq \varepsilon_{rev}/(2 + \varepsilon_{rev})$. For given reversible cycle qualities, the maximum cooling power and its corresponding COP are solely determined by the dissipation ratio δ . We note that as the dissipation at the high-temperature end diminishes ($\delta \rightarrow 1$), the cooling power diverges, whereas the COP approaches zero at this point. However, the product of the two is a constant, namely, $\lim_{\delta \rightarrow 1} (P_{max}\varepsilon_{MP}) = [W_{rev}\varepsilon_{rev}/(2\mathcal{L})]^2$, indicating that when the dissipation at the high-temperature heat reservoir is extremely small, the optimized extreme point moves along a hyperbola. In more specific case with two heat baths, one has $\eta_{rev} = \varepsilon_C = T_c/(T_h - T_c)$ and corresponding EMP is $\varepsilon_{MP} = \varepsilon_C/[2 + (1 - \delta)^{-1}\varepsilon_C]$, which is consistent with Ref. [22]. In Fig. 2(b), ε_{MP} as a function of δ with $T_c/T_h = 0.1, 0.5, 0.8$ is plotted as the curves below $\tilde{\eta}_{MP} \leq 0.5$, larger ε_C (larger T_c/T_h) leads to higher ε_{MP} .

PETORs for heat pumps and heat exchangers.— From Eq. (9), the PETOR of heat pump is (see Fig. 1)

$$P \leq \left(\frac{I_{rev}}{\mathcal{L}} \right)^2 \frac{\eta(\eta_{rev} - \eta)(\eta_{rev} - \delta)}{(\eta - \delta)^2}, \quad (17)$$

As we mentioned in remark iii) below Eq. (11), heat pumps and heat exchangers with $\theta\gamma < 0$ do not have locally maximum positive output power. The monotonicity of their PETORs can be directly observed from Fig. 1. Mathematically, $\theta\gamma < 0$ leads to P being a monotonically increasing function of cycle time τ in the physically meaningful region of $\tau > 0$, without any optimal time that locally maximizes P . This is also revealed in the specific analysis of heat pumps in Ref. [23].

It is worth noting that, in real world circumstance, practical heat exchangers usually do not have complete thermodynamic cycles; instead, they achieve rapid heat transfer by allowing the high-temperature substance in the heat exchanger to come into contact with the low-temperature environment to be heated though some medium [48, 49]. With thermodynamic cycles, the output mechanical work will reduce the heat release to the cold reservoir, thereby lowering the efficiency of the heat exchangers. However, local heat exchange around the heat exchanger may also lead to temperature non-uniformity in a relatively large space to be heated. It can be envisioned that by converting some heat into mechanical work, it is possible to perform work on the medium in the heated environment such as air, accelerating heat convection and achieving temperature uniformity. This analysis suggests that designing heat exchangers with adjustable mechanical output power (essentially a type of heat engine) to balance heat transfer efficiency and temperature uniformity in the heated environment is a practical task worth exploring, which has implications for guiding the optimal design of heat exchangers from the perspectives of engineering thermodynamics.

Summary.—We have obtained power-efficiency trade-off relation applicable to generic thermal machines. The core of our approach lies in two key points: i) unifying the performance description of different thermal machines using sign functions, and ii) establishing relations between total cycle dissipation, cycle time, and machine's power and efficiency, the trade off of which results from the lower bound on dissipation qualified by the thermodynamic length. Our results are applicable to cases with multiple heat baths as well as finite-sized heat reservoirs. Specifically, in the case of two heat reservoirs, by selecting appropriate cycle parameters, the presented general PETOR naturally recovers typical PETORs such as those for low-dissipation Carnot heat engines and Carnot refrigerators, and that for irreversible heat engines with finite-sized reservoirs. The EMP determined by our PETOR also recovers several existing results obtained case by case. Moreover, our work is highly generalizable (see remarks below Eq. (11)), Eq. (1) is applicable to any thermal machine driven by isothermal shortcut protocols [33], and the approach we use to derive PETOR can also be extended to study thermodynamic cycles that do not satisfy the $1/\tau$ -scaling of dissipation [36–40]. This study lays the foundation for a unified description of thermodynamic cycles and general approaches to thermal machine performance optimization.

Acknowledgment.—This work is supported by the National Natural Science Foundation of China for support under grant No. 12305037 and the Fundamental Research Funds for the Central Universities under grant No. 2023NTST017.

Appendix A: Thermodynamic geometry approach to finite-time Carnot cycle with ideal gas

In the following, we specifically demonstrate how to use thermodynamic geometric approach to determine the dissipation ratio δ in a finite-time Carnot cycle with an ideal gas as the working substance. When the gas with a molar amount of n and volume V is driven slowly in a hot reservoir of temperature T_h (finite-time high-temperature isothermal process of duration τ_h), the gas pressure p reads [12]

$$p = p_q - \frac{T_h}{\kappa_h} \left(\frac{nR}{V} \right)^2 \dot{V}, \quad (\text{A1})$$

where p_q is the gas pressure in quasi-static process ($\dot{V} \rightarrow 0$), κ_h is the heat transfer coefficient between the gas and the reservoir, and R is the ideal gas constant. According to Ref. [39],

$$\begin{aligned} \mathcal{L}_h &= \int_0^{\tau_1} \sqrt{\dot{W}_{\text{ex}}(t)} dt = \int_0^{\tau_1} \sqrt{p_{\text{ex}}(t)} \dot{V} dt \\ &= \left| \int_{V_0}^{V_f} \sqrt{\frac{T_h}{\kappa_h}} \frac{nR dV}{V} \right| = nR \sqrt{\frac{T_h}{\kappa_h}} \left| \ln \left(\frac{V_f}{V_0} \right) \right|, \end{aligned}$$

where $p_{\text{ex}} \equiv |p - p_q|$ has been used. Thus, the corresponding dissipation in this process follows as [50]

$$Q_{\text{ir}}^h \geq \frac{\mathcal{L}_h^2}{\tau_h} = \frac{T_h [nR \ln(V_f/V_0)]^2}{\kappa_h \tau_h}. \quad (\text{A2})$$

Similarly, in the low-temperature finite-time isothermal process of duration τ_c

$$Q_{\text{ir}}^c \geq \frac{\mathcal{L}_c^2}{\tau_c} = \frac{T_c [nR \ln(V_f/V_0)]^2}{\kappa_c \tau_c}. \quad (\text{A3})$$

For the whole cycle, the minimal dissipation is [11, 33]

$$A_{\min}(\tau = \tau_h + \tau_c) = \frac{(\mathcal{L}_h + \mathcal{L}_c)^2}{\tau_h + \tau_c}. \quad (\text{A4})$$

It is easily checked that

$$\begin{aligned} &\frac{\mathcal{L}_h^2}{\tau_h} + \frac{\mathcal{L}_c^2}{\tau_c} - \frac{(\mathcal{L}_h + \mathcal{L}_c)^2}{\tau_h + \tau_c} \\ &= \frac{\mathcal{L}_h^2 \tau_c (\tau_h + \tau_c) + \mathcal{L}_c^2 \tau_h (\tau_h + \tau_c) - (\mathcal{L}_h + \mathcal{L}_c)^2 \tau_h \tau_c}{\tau_h \tau_c (\tau_h + \tau_c)} \\ &= \frac{(\mathcal{L}_h \tau_c - \mathcal{L}_c \tau_h)^2}{\tau_h \tau_c (\tau_h + \tau_c)} \geq 0, \end{aligned}$$

namely, the total dissipation $A = A_h + A_c \geq A_{\min}$. Here, the equal sign is taken when

$$A_h = \frac{\mathcal{L}_h^2}{\tau_h}, \quad A_c = \frac{\mathcal{L}_c^2}{\tau_c}, \quad \frac{\mathcal{L}_h}{\mathcal{L}_c} = \frac{\tau_h}{\tau_c}, \quad (\text{A5})$$

which is specifically written, for ideal gas, as

$$\frac{A_h}{A_c} = \frac{\mathcal{L}_h}{\mathcal{L}_c} = \frac{\tau_h}{\tau_c} = \sqrt{\frac{T_h \kappa_c}{T_c \kappa_h}}. \quad (\text{A6})$$

Therefore, we obtain

$$\delta = \frac{\mathcal{L}_h}{\mathcal{L}} = \frac{1}{1 + \sqrt{\frac{T_c \kappa_h}{T_h \kappa_c}}}. \quad (\text{A7})$$

Since $\kappa_h/\kappa_c \in (0, \infty)$, one has $\delta \in (0, 1)$. Especially, in the symmetric case with $\kappa_h/\kappa_c = 1$, it follows from Eq. (13) that $\eta_{\text{MP}} = 1 - \sqrt{1 - \eta_C}$, which is exactly the Curzon-Ahlborn efficiency [15]

Appendix B: Upper and lower bound for efficiency at given power

The range of efficiency at maximum power indicates a varying trade-off relation in heat engines as a function of the dissipation ratio, allowing us to establish tighter overall upper and lower bounds of efficiency at given power from Eq. (12)

$$\frac{\tilde{\eta}(1 - \tilde{\eta})}{(1 - \delta \eta_{\text{rev}} \tilde{\eta})^2} \geq \frac{\tilde{P}}{4(1 - \delta \eta_{\text{rev}})} \equiv \lambda, \quad (\text{B1})$$

namely,

$$(1 + \lambda \delta^2 \eta_{\text{rev}}^2) \tilde{\eta}^2 - (1 + 2\lambda \delta \eta_{\text{rev}}) \tilde{\eta} + \lambda \leq 0. \quad (\text{B2})$$

The solution of the above inequality of $\tilde{\eta}$ are

$$\tilde{\eta}_{\pm} = \frac{(1 + 2\lambda \delta \eta_{\text{rev}}) \pm \sqrt{4\lambda \delta \eta_{\text{rev}} + 1 - 4\lambda}}{2(\lambda \delta^2 \eta_{\text{rev}}^2 + 1)}. \quad (\text{B3})$$

Under the condition that the power and thermodynamic parameters are fixed, $\tilde{\eta}_{\pm}$ delineate the upper and lower bounds of the low-dissipation region. Generally, precise knowledge of the heat engine parameters is elusive; hence, deriving a universal upper/lower bounds that are valid for all δ within this range is of practical significance. Next, we prove the monotonic increasing nature of the tight upper and lower bounds for efficiency, as a function of a given power with a variable parameter δ .

To investigate the monotonicity of this function, we differentiate it with respect to δ , yielding the following equation

$$\tilde{\eta}_- = \frac{(1 + 2\lambda \delta \eta_{\text{rev}}) - \sqrt{4\lambda \delta \eta_{\text{rev}} + 1 - 4\lambda}}{2(\lambda \delta^2 \eta_{\text{rev}}^2 + 1)}, \quad (\text{B4})$$

such that

$$\frac{d\tilde{\eta}_-}{d\delta} = \frac{-\eta_{\text{rev}} \tilde{P} (a_- x^2 + b_- x - 4)}{(\tilde{P} x^2 - 4x + 4)^2}, \quad (\text{B5})$$

where $a_- = \tilde{P} + 2\sqrt{1 - \tilde{P}} - 2$, $b_- = 4 - 4\sqrt{1 - \tilde{P}}$, $x = \delta \eta_{\text{rev}}$. The sign of the above equation is determined by $a_- x^2 + b_- x - 4$. Notably, it is straightforward to observe that $a_- \leq 0$, with equality holding only when $\tilde{P} = 1$. Furthermore, under the condition $\Delta = b_-^2 + 16a_- = 0$, we find that $a_- x^2 + b_- x - 4 \leq 0$ for $\tilde{P} \neq 1$. When $\tilde{P} = 1$ both a_- and b_- vanish, reducing the quadratic expression as -4 . We conclude that $\frac{d\tilde{\eta}_-}{d\delta} > 0$ for

$\delta \in [0, 1]$. Thus, the overall lower bound is reached at $\delta = 0$, substituting which into Eq. (B5) yields $\tilde{\eta}_L = (1 - \sqrt{1 - \tilde{P}})/2$. Similarly, for

$$\tilde{\eta}_+ = \frac{(1 + 2\lambda\delta\eta_{\text{rev}}) + \sqrt{4\lambda\delta\eta_{\text{rev}} + 1 - 4\lambda}}{2(\lambda\delta^2\eta_{\text{rev}}^2 + 1)}, \quad (\text{B6})$$

one has

$$\frac{d\tilde{\eta}_+}{d\delta} = \frac{-\eta_{\text{rev}}\tilde{P}(a_+x^2 + b_+x - 4)}{(\tilde{P}x^2 - 4x + 4)^2}, \quad (\text{B7})$$

where $a_+ = \tilde{P} - 2\sqrt{1 - \tilde{P}} - 2$, $b_+ = 4 + 4\sqrt{1 - \tilde{P}}$, $x = \delta\eta_{\text{rev}}$. The sign of the above equation is determined by $a_+x^2 + b_+x - 4$. Notably, it is straightforward to observe that $a_+ < 0$. Furthermore, under the condition $\Delta = b_+^2 + 16a_+ = 0$, we find that $a_+x^2 + b_+x - 4 \leq 0$. In summary, we conclude that $\frac{d\tilde{\eta}_+}{d\delta} \geq 0$ for $\delta \in [0, 1]$. Therefore, the overall upper bound $\tilde{\eta}_U \geq \tilde{\eta}$ is achieved with $\delta = 1$, substituting which into Eq. (B6), Eq. (14) is obtained.

-
- [1] A. Bejan, *Advanced Engineering Thermodynamics*, 4th ed. (Wiley, Hoboken, 2016).
- [2] R. S. Berry, P. Salamon, and B. Andresen, eds., *Finite-Time Thermodynamics* (MDPI - Multidisciplinary Digital Publishing Institute, 2022).
- [3] L. Chen and Z. Yan, The effect of heat-transfer law on performance of a two-heat-source endoreversible cycle, *J. Chem. Phys.* **90**, 3740 (1989).
- [4] V. Holubec and A. Ryabov, Efficiency at and near maximum power of low-dissipation heat engines, *Phys. Rev. E* **92**, 052125 (2015).
- [5] N. Shiraishi, K. Saito, and H. Tasaki, Universal trade-off relation between power and efficiency for heat engines, *Phys. Rev. Lett.* **117**, 190601 (2016).
- [6] V. Holubec and A. Ryabov, Maximum efficiency of low-dissipation heat engines at arbitrary power, *J. Stat. Mech.-Theory Exp.* **2016**, 073204 (2016).
- [7] Y.-H. Ma, D. Xu, H. Dong, and C.-P. Sun, Universal constraint for efficiency and power of a low-dissipation heat engine, *Phys. Rev. E* **98**, 042112 (2018).
- [8] P. Pietzonka and U. Seifert, Universal Trade-Off between Power, Efficiency, and Constancy in Steady-State Heat Engines, *Phys. Rev. Lett.* **120**, 190602 (2018).
- [9] H. Yuan, Y.-H. Ma, and C. P. Sun, Optimizing thermodynamic cycles with two finite-sized reservoirs, *Phys. Rev. E* **105**, L022101 (2022).
- [10] T.-J. Zhou, Y.-H. Ma, and C. Sun, Finite-time optimization of a quantum szilard heat engine, *Phys. Rev. Res.* **6**, 043001 (2024).
- [11] K. Brandner and K. Saito, Thermodynamic Geometry of Microscopic Heat Engines, *Phys. Rev. Lett.* **124**, 040602 (2020).
- [12] Y.-H. Ma, R.-X. Zhai, J. Chen, C. P. Sun, and H. Dong, Experimental Test of the $1/\tau$ -Scaling Entropy Generation in Finite-Time Thermodynamics, *Phys. Rev. Lett.* **125**, 210601 (2020).
- [13] R.-X. Zhai, F.-M. Cui, Y.-H. Ma, C. P. Sun, and H. Dong, Experimental test of power-efficiency trade-off in a finite-time Carnot cycle, *Phys. Rev. E* **107**, L042101 (2023).
- [14] Z. C. Tu, Efficiency at maximum power of feynman's ratchet as a heat engine, *J. Phys. A: Math. Theor.* **41**, 312003 (2008).
- [15] F. L. Curzon and B. Ahlborn, Efficiency of a carnot engine at maximum power output, *Am. J. Phys.* **43**, 22 (1975).
- [16] C. Van den Broeck, Thermodynamic efficiency at maximum power, *Phys. Rev. Lett.* **95**, 190602 (2005).
- [17] M. Esposito, R. Kawai, K. Lindenberg, and C. Van den Broeck, Efficiency at maximum power of low-dissipation carnot engines, *Phys. Rev. Lett.* **105**, 150603 (2010).
- [18] C. H. Blanchard, Coefficient of performance for finite speed heat pump, *Journal of Applied Physics* **51**, 2471 (1980).
- [19] L. G. Chen, F. Sun, and C. S. Wu, The influence of heat-transfer law on the endo-reversible carnot refrigerator, *Journal of The Institute of Energy* **69**, 96 (1996).
- [20] Y. Wang, M. Li, Z. C. Tu, A. C. Hernández, and J. M. M. Roco, Coefficient of performance at maximum figure of merit and its bounds for low-dissipation Carnot-like refrigerators, *Phys. Rev. E* **86**, 011127 (2012).
- [21] Y. Izumida, K. Okuda, A. Calvo Hernández, and J. M. M. Roco, Coefficient of performance under optimized figure of merit in minimally nonlinear irreversible refrigerator, *Europhys. Lett.* **101**, 10005 (2013).
- [22] V. Holubec and Z. Ye, Maximum efficiency of low-dissipation refrigerators at arbitrary cooling power, *Phys. Rev. E* **101**, 052124 (2020).
- [23] Z. Ye and V. Holubec, Maximum efficiency of low-dissipation heat pumps at given heating load, *Phys. Rev. E* **105**, 024139 (2022).
- [24] W. Z. Chen, F. R. Sun, S. M. Cheng, and L. G. Chen, Study on optimal performance and working temperatures of endoreversible forward and reverse carnot cycles, *International Journal of Energy Research* **19**, 751 (1995).
- [25] C. De Tomás, J. Roco, A. C. Hernández, Y. Wang, and Z. Tu, Low-dissipation heat devices: Unified trade-off optimization and bounds, *Phys. Rev. E* **87**, 012105 (2013).
- [26] R. S. Johal, Performance optimization of low-dissipation thermal machines revisited, *Phys. Rev. E* **100**, 052101 (2019).
- [27] J. Gonzalez-Ayala, A. Medina, J. M. M. Roco, and A. C. Hernández, Entropy generation and unified optimization of Carnot-like and low-dissipation refrigerators, *Phys. Rev. E* **97**, 022139 (2018).
- [28] H. S. Leff and W. D. Teeters, EER, COP, and the second law efficiency for air conditioners, *Am. J. Phys.* **46**, 19 (1978).
- [29] J. Gordon, K. Ng, and H. Chua, Optimizing chiller operation based on finite-time thermodynamics: Universal modeling and experimental confirmation, *International Journal of Refrigeration* **20**, 191 (1997).
- [30] Conventionally, heat exchangers are described with heat transfer processes rather than complete thermodynamic cycles. To ensure the completeness of Tab. 1 with respect to θ and γ , we have included them accordingly. Our general definition of efficiency is consistent with that of the heat exchangers in thermodynamic engineering [48, 49].
- [31] This additivity of dissipation is jointly induced by the first and second laws of thermodynamics. Taking a heat engine cycle as an example, we have $Q^h - Q^c = W$ and $Q_{\text{rev}}^h - Q_{\text{rev}}^c = W_{\text{rev}}$. Subtract the above two equations yields $(Q_{\text{rev}}^h - Q^h) + (Q^c - Q_{\text{rev}}^c) = W_{\text{rev}} - W$, which can be further simplified as $Q_{\text{ir}}^h + Q_{\text{ir}}^c = W_{\text{ir}}$.
- [32] G. Li, J.-F. Chen, C. P. Sun, and H. Dong, Geodesic Path for the

- Minimal Energy Cost in Shortcuts to Isothermality, *Phys. Rev. Lett.* **128**, 230603 (2022).
- [33] J.-F. Chen, Optimizing brownian heat engine with shortcut strategy, *Phys. Rev. E* **106**, 054108 (2022).
- [34] Y. Izumida and K. Okuda, Work Output and Efficiency at Maximum Power of Linear Irreversible Heat Engines Operating with a Finite-Sized Heat Source, *Phys. Rev. Lett.* **112**, 180603 (2014).
- [35] G. Li, H. T. Quan, and Z. C. Tu, Shortcuts to isothermality and nonequilibrium work relations, *Phys. Rev. E* **96**, 012144 (2017).
- [36] Y. Wang and Z. C. Tu, Bounds of efficiency at maximum power for normal-, sub-and super-dissipative carnot-like heat engines, *Commun. Theor. Phys.* **59**, 175 (2013).
- [37] J.-F. Chen, C.-P. Sun, and H. Dong, Achieve higher efficiency at maximum power with finite-time quantum otto cycle, *Phys. Rev. E* **100**, 062140 (2019).
- [38] N. Pancotti, M. Scandi, M. T. Mitchison, and M. Perarnau-Llobet, Speed-ups to isothermality: Enhanced quantum thermal machines through control of the system-bath coupling, *Phys. Rev. X* **10**, 031015 (2020).
- [39] J.-F. Chen, C. Sun, and H. Dong, Extrapolating the thermodynamic length with finite-time measurements, *Phys. Rev. E* **104**, 034117 (2021).
- [40] Y.-H. Ma, C. Sun, and H. Dong, Consistency of optimizing finite-time carnot engines with the low-dissipation model in the two-level atomic heat engine, *Commun. Theor. Phys.* **73**, 125101 (2021).
- [41] J.-F. Chen, R.-X. Zhai, C. Sun, and H. Dong, Geodesic lower bound of the energy consumption to achieve membrane separation within finite time, *PRX Energy* **2**, 033003 (2023).
- [42] A. Rolandi, P. Abiuso, and M. Perarnau-Llobet, Collective Advantages in Finite-Time Thermodynamics, *Phys. Rev. Lett.* **131**, 210401 (2023).
- [43] S. Liang, Y.-H. Ma, D. M. Busiello, and P. D. L. Rios, A minimal model for carnot efficiency at maximum power, arXiv preprint arXiv:2312.02323 [10.48550/arXiv.2312.02323](https://arxiv.org/abs/10.48550/arXiv.2312.02323) (2023).
- [44] Y. Izumida, Irreversible efficiency and carnot theorem for heat engines operating with multiple heat baths in linear response regime, *Phys. Rev. Res.* **4**, 023217 (2022).
- [45] C. Van den Broeck, Efficiency at maximum power in the low-dissipation limit, *Europhys. Lett.* **101**, 10006 (2013).
- [46] M. J. Ondrechen, B. Andresen, M. Mozurkewich, and R. S. Berry, Maximum work from a finite reservoir by sequential Carnot cycles, *Am. J. Phys.* **49**, 681 (1981).
- [47] Y.-H. Ma, Effect of Finite-Size Heat Source's Heat Capacity on the Efficiency of Heat Engine, *Entropy* **22**, 1002 (2020).
- [48] A. Bejan, General criterion for rating heat-exchanger performance, *International Journal of Heat and Mass Transfer* **21**, 655 (1978).
- [49] D. P. Sekulić and R. K. Shah, *Fundamentals of Heat Exchanger Design*, 1st ed. (Wiley, 2023).
- [50] P. Salamon and R. S. Berry, Thermodynamic Length and Dissipated Availability, *Phys. Rev. Lett.* **51**, 1127 (1983).